Propagation of Near-Limit Gaseous Detonations in Rough Walled Tubes

Tianfei Ren[1,2*], Yiran Yan[2,3*], Huanjuan Zhao[3], John H.S. Lee[2†] and Hoi Dick Ng[4]

[1] State Key Laboratory of Explosion Science and Technology, Beijing Institute of Technology, Beijing, 100081, China

[2] Department of Mechanical Engineering, McGill University, Montreal, QC, H3A 0C3, Canada

[3] State Key Laboratory of Ministry of Education of High-Efficient Mining and Safety of Metal Mines, University of Science and Technology Beijing, Beijing, 100083, China

[4] Department of Mechanical, Industrial and Aerospace Engineering, Concordia University, Montreal, QC, H3G 1M8, Canada

[†]Corresponding Author

Department of Mechanical Engineering
McGill University
817 Rue Sherbrooke Ouest
Montreal, QC, H3A 0C3,
Canada
E-mail: john.lee@mcgill.ca

Final manuscript submitted to *Shock Waves Journal*

May, 2020

[*] T. Ren and Y. Yan contributed equally and should be regarded as co-first authors.

Propagation of Near-Limit Gaseous Detonations in Rough Walled Tubes

by

Tianfei Ren, Yiran Yan, Huanjuan Zhao, John H.S. Lee and Hoi Dick Ng

Abstract

In this study, experiments were carried out to investigate the detonation velocity behavior near limits in rough walled tubes. The wall roughness was introduced by using different spiral inserts in 76.2-mm-diameter, 50.8-mm-diameter, 38.1-mm-diameter and 25.4-mm-diameter tubes. Different pre-mixed mixtures, $CH_4 + 2O_2$, $C_2H_2 + 2.5O_2$, $C_2H_2 + 2.5O_2 + 70\%Ar$ and $2H_2 + O_2$ were tested in the experiments. Different spiral wire diameters were used, and the pitch of each spiral was twice of the diameter to keep the same level of roughness in all experiments for each tube. Fiber optics were used to record the detonation time-of-arrival to deduce the velocity. The normalized velocity V/V_{CJ} and the velocity deficit δ were computed and analyzed to describe the detonation behavior near the limit. The cellular structure near the limit was recorded by the smoked foils.

Keywords: Detonation limit; Wall roughness; Spring inserts; Velocity deficit; Velocity fluctuation; Smoked foils

1. Introduction

Detonation limits refer to the conditions outside of which self-sustained propagation of a detonation wave is not possible [1]. Experimentally detonation limits can be brought about by too lean or too rich a mixture composition, reduction in the initial pressure, increase in the concentration of an inert diluent, reduction in the tube diameter, and high concentration of a chemical inhibitor. In general, as the limits are approached, the detonation velocity decreases and the unstable cellular structure is driven to lower modes, i.e., from multi-headed to single-headed spinning detonations. Wall roughness has been found to have strong influence on both the propagation velocity as well as the structure of the detonation wave. In obstacle-filled tubes, the detonation velocity can be as low as half the Chapman-Jouguet (CJ) value. Photographic observations also indicate that the detonation structure can be significantly perturbed. Numerous investigations have been carried out in the past few decades on detonation propagation in obstacle-filled tubes, e.g., [2-4]. Usually, the obstacles are in the form of circular orifice plates spaced periodically at about one tube diameter apart along the length of the tube. The orifice diameter as well as the spacing of the orifice plates are of the order of the diameter of the tube itself. Thus, it is difficult to consider these orifice plates-filled tubes as rough walled tubes. Indeed, photographic observations indicate that the diffraction of the detonation through the orifice and reflections from the orifice plate and the tube wall of the diffracted front play major roles in the failure and ignition as the detonation propagates past the obstacles. It is appropriate to define rough walled tubes as those whose dimension of the wall roughness is small as compared to the tube diameter. In this way, the effect of the wall roughness creates only small perturbations on the detonation and the flow field associated with the detonation front.

In the original study by Laffitte [5], a strip of coarse sand paper inserted into the tube was used to create wall roughness. In a later study by Shchelkin [6], a long length of a spiral coiled wire inserted into the tube provided an easier way to generate wall roughness. The pioneering studies by Laffitte and Shchelkin may be considered the first genuine investigations of detonation propagation in a rough walled tube. Since both Laffitte and Shchelkin were concerned mainly with promoting DDT in rough walled tubes, relatively little information on detonation velocity and structure was obtained. The later study by Guénoche [7] contained more data on detonation velocity in tubes with wire spirals. However, Guénoche used only one mixture of $C_2H_2 + O_2$. Brochet [8] was the first to obtain streak schlieren photographs of detonation propagation in tubes with spiral coils inserted. He reported the important result that the spiral coil tends to drive the detonation to lower unstable modes. However, Brochet used only mixtures of $C_2H_2 + 5O_2 + z{\cdot}N_2$ with various nitrogen concentrations. Teodorczyk *et al.* [9-11] also obtained framing schlieren photographs of detonations in $2H_2 + O_2$ mixture in a two-dimensional equivalent of a spiral coil in a channel. Some recent studies on detonation limits in rough walled tubes were also carried out, e.g., Starr *et al.* [12] and Zhang [13]. In the present paper, extensive information on detonation limits in rough walled tubes are reported. A variety of explosive mixtures, tube diameter as well as spiral geometric parameters were considered.

2. Experimental Details and Measurement

A generic schematic of the experimental apparatus arrangement is shown in Fig. 1. Three experimental setups with different scales were used. The first apparatus consists of 4 different inner-diameter (D) brass tubes, each 1.5 m long. The driver section has D = 25.4 mm and 38 mm, and the test section has D = 38.1 mm and 50.8 mm. The second consists of three 1.5-m-long, 25.4-

mm-diameter polycarbonate tubes. The third consists of a 1.2-m-long steel tube as the driver section and a 1.8-m-long polycarbonate tube as the test section, the tube diameter of the driver section and the test section is 76.2 mm. In all tubes, a Shchelkin spiral was put near the ignitor to facilitate detonation formation.

Pre-mixed stoichiometric mixtures of $2H_2 + O_2$, $C_2H_2 + 2.5O_2$, $C_2H_2 + 2.5O_2 + 70\%Ar$ and $CH_4 + 2O_2$ were used. Gaseous detonation dynamics, including initiation and propagation limits, are known to be affected by the inherent instability of the detonation structure. The four fuel/O_2 mixtures tested in this work are commonly used in laboratory-scale studies to cover a wide range of detonation instability, from very stable ones with regular cellular patterns (e.g., $C_2H_2 + 2.5O_2 + 70\%Ar$) to highly unstable mixtures with irregular cellular structure (e.g., $CH_4 + 2O_2$). It is worth mentioning that not all the mixtures were studied in the different diameter tubes and spiral parameters to reduce the number of experiments. The spirals are made of wire with diameter of 1 mm, 2 mm, 3 mm for the 25.4-mm-diameter tube, 1.5 mm, 3 mm, 5 mm, 6.5 mm for the 38.1-mm-diameter tube, 1.5 mm, 3 mm, 6.2 mm and 9 mm for the 50.8-mm-diameter tube, 9 mm and 11 mm for the 76.2-mm-diameter tube. The pitch of the spiral is double of the wire diameter. The length of the spiral in the rough section is 1.5 m long for all setups. For the less sensitive mixtures (e.g., $C_2H_2 + 2.5O_2 + 70\%Ar$), detonation initiation sometimes required the use of a driver section where a small slug of more sensitive $C_2H_2 + O_2$ mixture was used. Velocity measurements are carried out using optical fibers spaced at regular intervals along the tube, terminating at a photodiode (IF-950C). From the time-of-arrival data, detonation trajectories are obtained from which the averaged detonation velocity can be determined from the slope of the *x-t* trajectory. The detonation cellular structure is recorded on a rectangular strip of glass plate inserted across the diameter of the tube when the cell number is large. When the glass plate starts to have an influence

on the cellular structure and a longer measurement length is needed, a smoked Mylar foil inserted into the tube is used around the inner circumference.

3. Results and Discussion

From the time-of-arrival data measured by the photodiodes, the detonation wave trajectory can be plotted from which the averaged detonation velocity can be determined from the slope. For illustration, Fig. 2a-e shows typical trajectories for $C_2H_2 + 2.5O_2$ in a 25.4-mm-diameter tube, $C_2H_2 + 2.5O_2$ in a 76.2-mm-diameter tube, $CH_4 + 2O_2$ in a 50.8-mm-diameter tube, $C_2H_2 + 2.5O_2 +$ 70%Ar in a 50.8-mm-diameter tube and $2H_2 + O_2$ in a 50.8-mm-diameter tube, respectively. For each plot, the origin $x = 0$ denotes the location of the ignitor at the left end of the apparatus, regardless of whether there is a driver tube section or not. The vertical line shown in the plots defines separation between the initially smooth section of the tube from the rough section where the wire spiral coil is inserted. The slope of the trajectory was obtained to determine the averaged propagation velocity of the detonation in both the smooth section and the rough section. The change in the slope of the trajectory indicates the decrease in the detonation velocity in the rough section. For decreasing initial pressures, the velocity deficit in the rough section increases. For high initial pressures (hence more detonable mixtures), the velocity in the rough section is found to be constant. However, for lower initial pressure, e.g., $P_0 = 2$ kPa in Fig. 2a, the detonation velocity is seen to decay as it propagates along the rough section.

Figure 3a-d shows the detonation velocities in both the smooth and the rough section downstream of $C_2H_2 + 2.5O_2$ in the tubes of 25.4 mm, 38.1 mm, 50.8 mm and 76.2 mm diameter, respectively. For high initial pressures the velocity deficits are small, typically of the order of 90%V_{CJ} in the smooth section of the tube. For increasing roughness, i.e., larger wire diameter of

the spiral, the velocity deficits are larger. Generally, the decrease in detonation velocity with decreasing initial pressure is relatively small until near the limits where the velocity rapidly drops. The near-limit velocity is also not steady and a large variation is observed in different experiments. Following previous studies [12-17], the abrupt velocity drop is used as the criterion to define the detonation limits. As shown in the later section, the abrupt velocity deficit corresponds well to the disappearance of cellular detonation pattern signifying failure.

The normalized velocity results of $CH_4 + 2O_2$, $C_2H_2 + 2.5O_2 + 70\%Ar$ and $2H_2 + O_2$ in 38.1-mm, 50.8-mm and 76.2-mm-diameter tubes are given in Fig. 4a-g. Similarly, the velocity is of the order of $90\%V_{CJ}$ in the smooth section and drops suddenly when the initial pressure is lowered, both in smooth and rough sections. The boundary layer effect is more predominant with decreasing tube diameter, as Figs. 4a and 4b show, the limit for $CH_4 + 2O_2$ is about 5.5 kPa in the 38.1-mm-diameter smooth tube but 4.5 kPa in the 50.8-mm-diameter one. In addition, the velocity of $CH_4 + 2O_2$ is found to be unsteady near the limit and the experiments need be repeated more times to obtain a meaningful average as compared to the mixture $C_2H_2 + 2.5O_2 + 70\%Ar$ because $CH_4 + 2O_2$ is a very unstable mixture. Overall, the $2H_2 + O_2$ mixture has a similar qualitatively velocity deficit behavior, i.e., the velocity deficit increases as it approaches to the limits.

It is worth noting that at the limit (abrupt velocity drop, as denoted by the dashed lines), for some mixtures a fast deflagration or shock-flame complex can result and propagate at a relatively constant low velocity, as indicated in some cases by data points on the left of the dashed lines. These low velocity waves could be supported by various mechanisms, such as, the boundary layer effect in small diameter tubes, turbulence or compression wave fluctuations generated by the rough wall tube and the inherent instability of the combustible mixture [12, 13, 18, 19]. Due to the limitation of experimental diagnostics and the length of the test section used in this study, this

wave propagation regime cannot be fully analyzed and is beyond the scope of this work. When the initial pressure is lower than the limit at which the steady detonation begins to fail, the velocity could also fluctuate significantly. The photodiode signal sometimes becomes erratic and also cannot be triggered due to low luminosity of these low-velocity reactive waves.

The local detonation velocity can be determined from the time interval between two photo probes. Thus, the velocity fluctuation can be computed as $\delta = |V_l - V_m|/V_m$ where V_l is the local detonation velocity and V_m the average velocity over the length of propagation of the detonation along the tube. Apart from the abrupt increase of velocity deficit as shown in Figs. 3 and 4, the level of velocity fluctuation provides another method to detect the onset of detonation limits. Figure 5 shows the variation of the maximum velocity fluctuation δ for the mixtures $C_2H_2 + 2.5O_2$ with initial pressures in all the different tubes and spiral parameters (wire diameter). For completeness, the velocity fluctuation results obtained for other mixtures, i.e., $CH_4 + 2O_2$, $C_2H_2 + 2.5O_2 + 70\%Ar$ and $2H_2 + O_2$ are also given in Fig. 6. In general, at high initial pressures, the velocity fluctuations are relatively small (less than 0.1) but increase as the initial pressure is decreased towards the limits. Again, experiments for $CH_4 + 2O_2$ need repeated tests when the initial pressure is near the limit because of the instability. For all the mixtures, the velocity fluctuations increase rapidly in the pressure range of the limits. This behavior is in accord with velocity results of Figs. 3 and 4, when the limits are approached large variation in the mean velocity is observed. With increasing roughness, the limit shifts to a higher initial pressure. The use of velocity fluctuations to define detonation limits was first proposed by Manson *et al.* [20]. He recognized the unstable nature of the detonation as the limits are approached and set an arbitrary value for the velocity fluctuation of $\delta < 0.004$ (i.e., 0.4%) as the maximum allowable deviation from the mean for stable detonations. Manson's criterion is too restrictive and would exclude spinning detonations

even though these propagate at a relatively steady velocity. Hence, Manson only considers stable detonations with velocity very close to the CJ value to be within the limits.

In the study by Brochet [8] and also in the paper by Manson *et al.* [20] streak schlieren photographs were used to observe detonations in a tube with a spiral coil. The streak schlieren photographs revealed a strong influence on the structure of the detonation, particularly the spiral coil causes the cellular detonation to go to lower unstable modes. Past the lowest unstable mode of single-headed spinning detonation, no structure was observed even though periodic pressure fluctuations due to the interaction with the spiral coil can be identified. In this study, smoked foils were used to record the cellular structure. Figure 7 shows some typically smoked foil records of detonations propagating in rough-walled tubes with the spring coil for $C_2H_2 + 2.5O_2 + 70\%Ar$, $CH_4 + 2O_2$ and $2H_2 + O_2$ mixtures. At an initial pressure far from the limits, multi-headed cellular structure is recorded. It then evolves to single-headed spin-wave when initial pressure decreases approaching the limits. Further reduction in the initial pressure suppresses all unstable cellular structures and nothing is registered on the smoked foil, see for example the results for $P_0 = 9.8$ kPa in Fig. 7c. It is worth noting that the changes of cell patterns are essentially the same as in smooth tubes, see Fig. 8 for the smoked foil results of $C_2H_2 + 2.5O_2$ in two different diameter tubes. For near-limit detonation propagation in both smooth and rough tubes, the pictures show that smoked foils for multi-headed to single headed spin-wave compare well with the normalized velocity for indicating the changes of cellular structure near the limit.

When approaching the limit, the smoked foil can record single-head spin under a pressure which increases with the increasing roughness. In Fig. 9, for the 38.1-mm-diameter tube, single-headed records of the mixture $C_2H_2 + 2.5O_2$ are obtained under $P_0 = 1.2$ kPa in the smooth section, see Fig. 9a, and under $P_0 = 1.6$ kPa with a spiral coil of 6.5 mm wire diameter, see Fig. 9d. Based

on these smoked foil records, it is also found that for sensitive mixtures, the limit increases gradually higher with increasing roughness. For insensitive mixtures, however, the limit rises rapidly, e.g., for $C_2H_2 + 2.5O_2 + 70\%Ar$ in rough section with 1.5 mm wire diameter, the limit is 3.5 kPa. But in the rough section with 5 mm wire diameter, it changes to 7 kPa, see Figs. 9e and 9f.

4. Concluding Remarks

Numerous studies in the past focused on the use of repeated orifice plates as obstacles. It was found that local reflection and diffraction of the detonation front past the orifice plates dominate the failure and re-initiation mechanisms. The present study employs a spiral coil with wire diameter that is small as compared to the tube diameter. It is proposed that these tubes with spiral coil inserts simulate better a genuine rough walled tube than the large blockage repeated orifice plates. Indeed, the present results are found to differ from those using repeated orifice plates. Of particular importance in the present study is the demonstration that wall roughness tends to drive the cellular detonations towards more fundamental lower modes. At the limit, it is found that the detonation is devoid of cellular structure. This indicates that the development of cellular structure is essential for the self-sustaining propagation of detonation waves. Previous speculation of the role of obstacles to generate turbulence to sustain the propagation of detonations appear to be unsubstantiated. Whether in smooth or rough wall tubes, the ability of the detonation front to develop cellular instability is paramount to gaseous detonation propagation.

Acknowledgments

This work is supported by the Natural Sciences & Engineering Research Council of Canada (NSERC). T. Ren is funded by the International Graduate Exchange Program of Beijing Institute of Technology. Y. Yan is grateful for the financial support by the China Scholarship Council (CSC).

References

1. Lee, J.H.S.: The Detonation Phenomenon. Cambridge University Press, Cambridge (2008). https://doi.org/10.1017/CBO9780511754708
2. Gu, L.S., Knystautas, R., Lee, J.H.: Influence of obstacle spacing on the propagation of quasi-detonation. AIAA Prog. Astronaut. Aeronaut. 114, 232–247 (1988). https://doi.org/10.2514/5.9781600865886.0232.0247
3. Ciccarelli, G., Cross, M.: On the propagation mechanism of a detonation wave in a round tube with orifice plates. Shock Waves 26 (5), 587-597 (2016). https://doi.org/10.1007/s00193-016-0676-6
4. Ciccarelli, G., Wang, Z., Lu, J., Cross, M.: Effect of orifice plate spacing on detonation propagation. J. Loss Prev. Process Ind. 49, 739-744 (2017). https://doi.org/10.1016/j.jlp.2017.03.014
5. Laffitte, P.: Sur la formation de l'onde explosive. C. R. Acad. Sci. 176, 1392-1394 (1923).
6. Shchelkin, K.I.: Detonation of gases in rough tubes. Zh. Teknich. Fiz. SSSR. 17, 613-618 (1947).
7. Guénoche, H.: The detonation and deflagration of gas mixtures. Rev. Inst. Français Pétrole 4, 48-69 (1949).

8. Brochet, C.: Contribution à l'Etude des Détonations Instable dans les Mélanges Gazeux. PhD thesis, University of Poitiers, France, (1966).
9. Teodorczyk, A., Lee, J.H.S.: Detonation attenuation by foams and wire meshes lining the walls. Shock Waves 4, 225-236 (1995). https://doi.org/10.1007/BF01414988
10. Teodorczyk, A., Lee, J.H.S., Knystautas, R.: Propagation mechanism of quasi-detonations. Proc. Combust. Inst. 22, 1723-1731 (1988). https://doi.org/10.1016/S0082-0784(89)80185-7
11. Teodorczyk, A., Lee, J.H.S., Knystautas, R.: Photographic study of the structure and propagation mechanisms of quasi-detonations in rough tubes. AIAA Prog. Astronaut. Aeronaut. 133, 223-240 (1991). https://doi.org/10.2514/5.9781600866067.0223.0240
12. Starr, A., Lee, J.H.S., Ng, H.D.: Detonation limits in rough walled tubes. Proc. Combust. Inst. 35(2), 1989-1996 (2015). https://doi.org/10.1016/j.proci.2014.06.130
13. Zhang, B.: The influence of wall roughness on detonation limits in hydrogen–oxygen mixture. Combust. Flame 169, 333-339 (2016). https://doi.org/10.1016/j.combustflame.2016.05.003
14. Lee, J.H.S., Jesuthasan, A., Ng, H.D.: Near limit behavior of the detonation velocity. Proc. Combust. Inst. 34(2), 1957-1963 (2013). https://doi.org/10.1016/j.proci.2012.05.036
15. Gao, Y., Zhang, B., Ng, H.D., Lee, J.H.S.: An experimental investigation of detonation limits in hydrogen–oxygen–argon mixtures. Int. J. Hydrogen Energy 41(14), 6076-6083 (2016). https://doi.org/10.1016/j.ijhydene.2016.02.130
16. Gao, Y., Ng, H.D., Lee, J.H.S.: Minimum tube diameters for steady propagation of gaseous detonations. Shock Waves 24(4), 447-454 (2014). https://doi.org/10.1007/s00193-014-0505-8

17. Zhang, B., Shen, X., Pang, L., Gao, Y.: Detonation velocity deficits of H_2/O_2/Ar mixture in round tube and annular channels. Int. J. Hydrogen Energy 40(43), 15078-15087 (2015). https://doi.org/10.1016/j.ijhydene.2015.09.036
18. Manzhalei, V.I.: Detonation regimes of gases in capillaries. Combust. Expl. Shock Waves 28, 296-302 (1992). https://doi.org/10.1007/BF00749647
19. Camargo, A., Ng, H.D., Chao, J., Lee, J.H.S.: Propagation of near-limit gaseous detonations in small diameter tubes. Shock Waves 20(6), 499-508 (2010). https://doi.org/10.1007/s00193-010-0253-3
20. Manson, N., Brochet, C., Brossard, J., Pujol, Y.: Vibratory phenomena and instability of self-sustained detonations in gases. Proc. Combust. Inst. 9, 461–469 (1963). https://doi.org/10.1016/S0082-0784(63)80055-7

Figure Captions

Fig. 1 Sketch of the apparatus.

Fig. 2 Sample trajectories for $C_2H_2 + 2.5O_2$ in (a) 25.4-mm-diameter and (b) 76.2-mm-diameter tubes; for $CH_4 + 2O_2$ in (c) 50.8-mm-diameter tube; for $C_2H_2 + 2.5O_2 + 70\%Ar$ in (d) 50.8-mm-diameter tube; and for $2H_2 + O_2$ in (f) 50.8-mm-diameter tube.

Fig. 3 The normalized velocity for $C_2H_2 + 2.5O_2$ in (a) 25.4-mm-diameter, (b) 38.1-mm-diameter, (c) 50.8-mm-diameter and (d) 76.2-mm-diameter tubes.

Fig. 4 The normalized velocity for $CH_4 + 2O_2$ in (a) 38.1-mm-diameter and (b) 50.8-mm-diameter tubes; for $C_2H_2 + 2.5O_2 + 70\%Ar$ in (c) 38.1-mm-diameter, (d) 50.8-mm-diameter and (e) 76.2-mm-diameter tubes; and for $2H_2 + O_2$ in (f) 38.1-mm-diameter tube and (g) 50.8-mm-diameter tube.

Fig. 5 Velocity fluctuation as a function of initial pressure and spring diameters for $C_2H_2 + 2.5O_2$ in (a) 25.4-mm-diameter, (b) 38.1-mm-diameter, (c) 50.8-mm-diameter and (d) 76.2-mm-diameter tubes.

Fig. 6 Velocity fluctuation as a function of initial pressure and spring diameters for $CH_4 + 2O_2$ in (a) 38.1-mm-diameter and (b) 50.8-mm-diameter tubes; for $C_2H_2 + 2.5O_2 + 70\%Ar$ in (c) 38.1-mm-diameter, (d) 50.8-mm-diameter and (e) 76.2-mm-diameter tubes; and for $2H_2 + O_2$ in (f) 38.1-mm-diameter and (g) 50.8-mm-diameter tube.

Fig. 7 Smoked foils and the normalized velocity as a function of initial pressure for a) $C_2H_2 + 2.5O_2 + 70\%Ar$ with a 3 mm spring in 38.1-mm-diameter tube; (b) $CH_4 + 2O_2$ using a 5 mm spring in 38.1-mm-diameter tube; and (c) $2H_2 + O_2$ with a 6.2 mm spring in 50.8-mm-diameter tube.

Fig. 8 Smoked foils and the normalized velocity for $C_2H_2 + 2.5O_2$ in smooth tube of (a) 25.4 mm diameter and (b) 76.2 mm diameter.

Fig. 9 Smoked foils for $C_2H_2 + 2.5O_2$ in 38.1-mm-diameter tube with (a) P_0 = 1.2 kPa in smooth tube, (b) P_0 = 1.4 kPa with a 3 mm spring, (c) P_0 = 1.55 kPa with a 5 mm spring and (d) P_0 = 1.6 kPa with a 6.5 mm spring; Smoked foils for $C_2H_2 + 2.5O_2$ + 70%Ar in 38.1-mm-diameter tube with (e) P_0 = 3.5 kPa with a 1.5 mm spring and (f) P_0 = 7 kPa with a 5 mm spring.

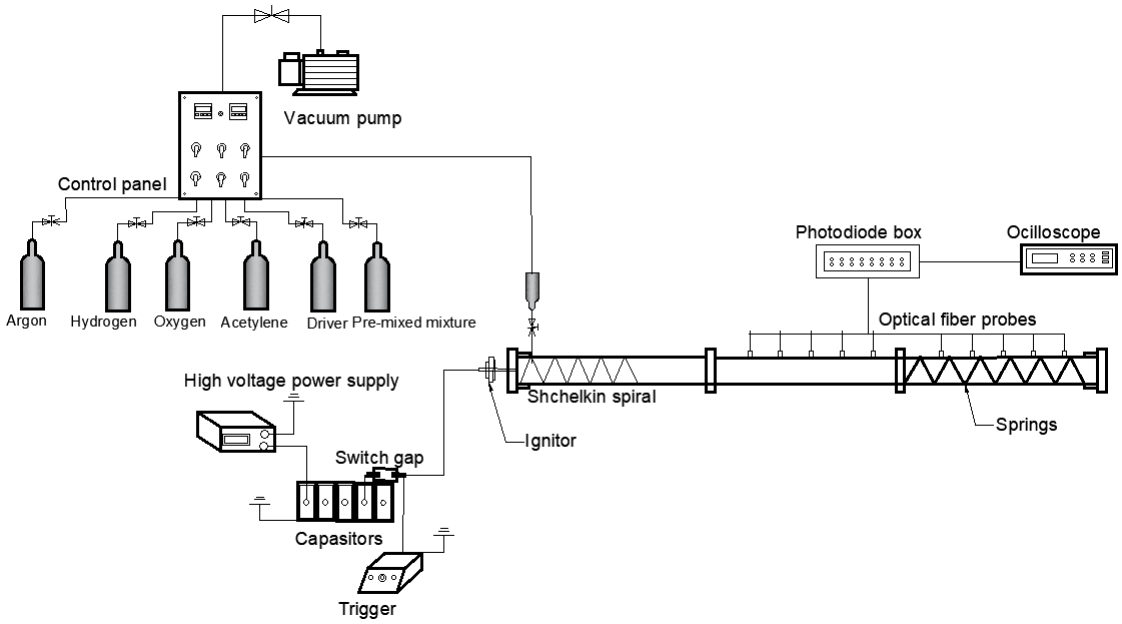

Fig. 1

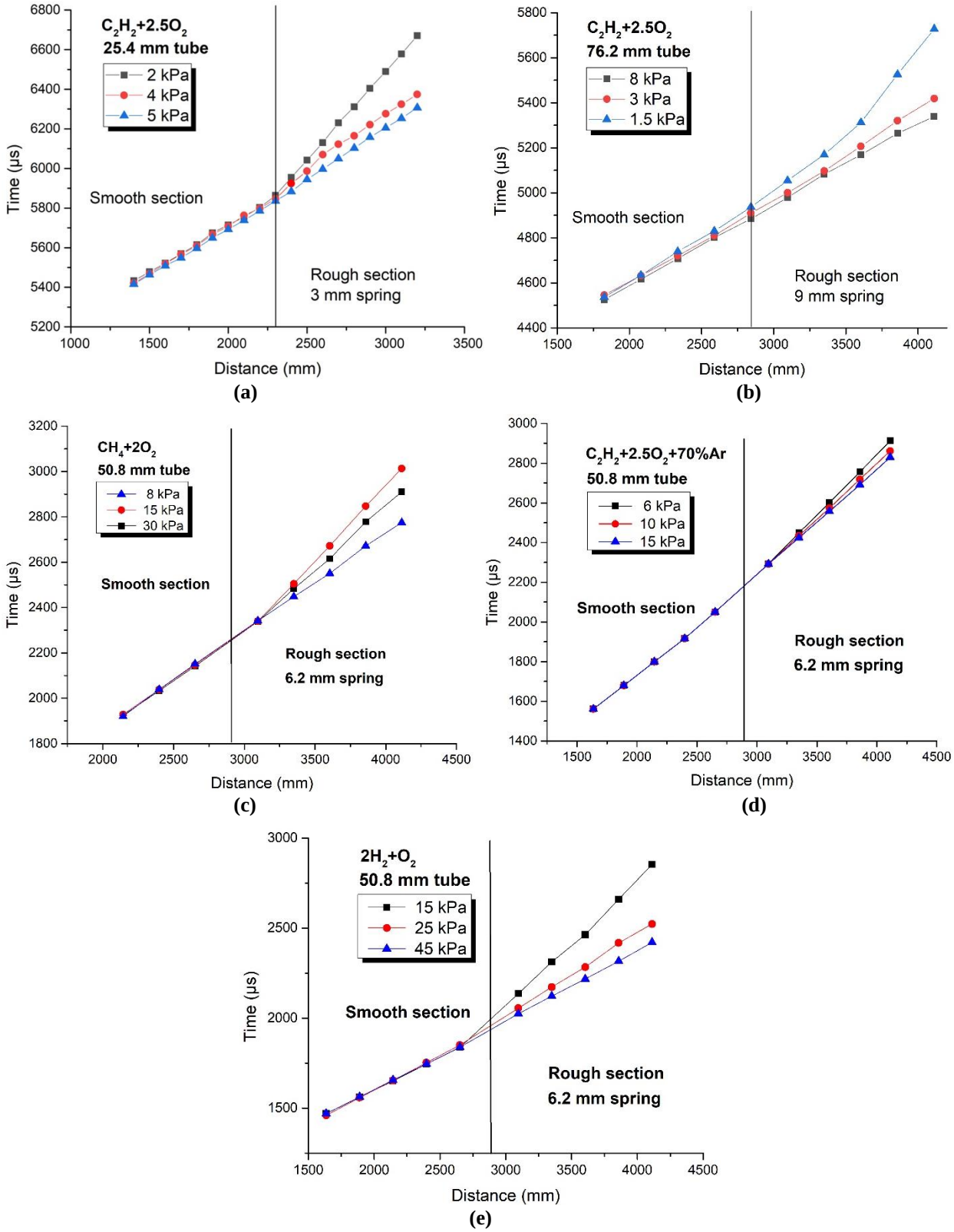
C2H2+2.5O2
25.4 mm tube
2 kPa
4 kPa
5 kPa
Smooth section
Rough section
3 mm spring
Time (μs)
Distance (mm)
(a)
C2H2+2.5O2
76.2 mm tube
8 kPa
3 kPa
1.5 kPa
Smooth section
Rough section
9 mm spring
Time (μs)
Distance (mm)
(b)
CH4+2O2
50.8 mm tube
8 kPa
15 kPa
30 kPa
Smooth section
Rough section
6.2 mm spring
Time (μs)
Distance (mm)
(c)
C2H2+2.5O2+70%Ar
50.8 mm tube
6 kPa
10 kPa
15 kPa
Smooth section
Rough section
6.2 mm spring
Time (μs)
Distance (mm)
(d)
2H2+O2
50.8 mm tube
15 kPa
25 kPa
45 kPa
Smooth section
Rough section
6.2 mm spring
Time (μs)
Distance (mm)
(e)

Fig. 2

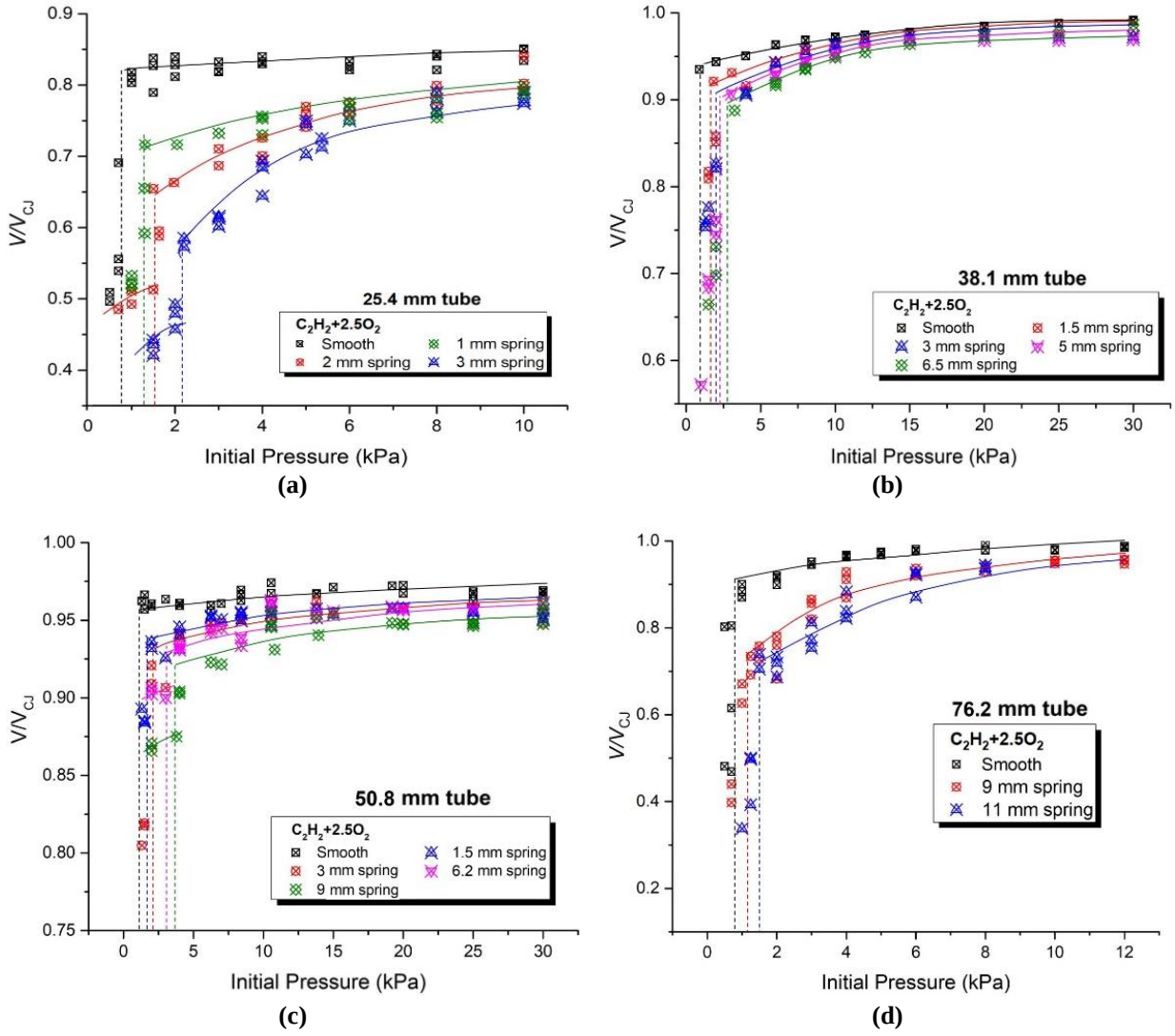
25.4 mm tube
C2H2+2.5O2
Smooth
1 mm spring
2 mm spring
3 mm spring
V/VCJ
Initial Pressure (kPa)
(a)
38.1 mm tube
C2H2+2.5O2
Smooth
1.5 mm spring
3 mm spring
5 mm spring
6.5 mm spring
V/VCJ
Initial Pressure (kPa)
(b)
50.8 mm tube
C2H2+2.5O2
Smooth
1.5 mm spring
3 mm spring
6.2 mm spring
9 mm spring
V/VCJ
Initial Pressure (kPa)
(c)
76.2 mm tube
C2H2+2.5O2
Smooth
9 mm spring
11 mm spring
V/VCJ
Initial Pressure (kPa)
(d)

Fig. 3

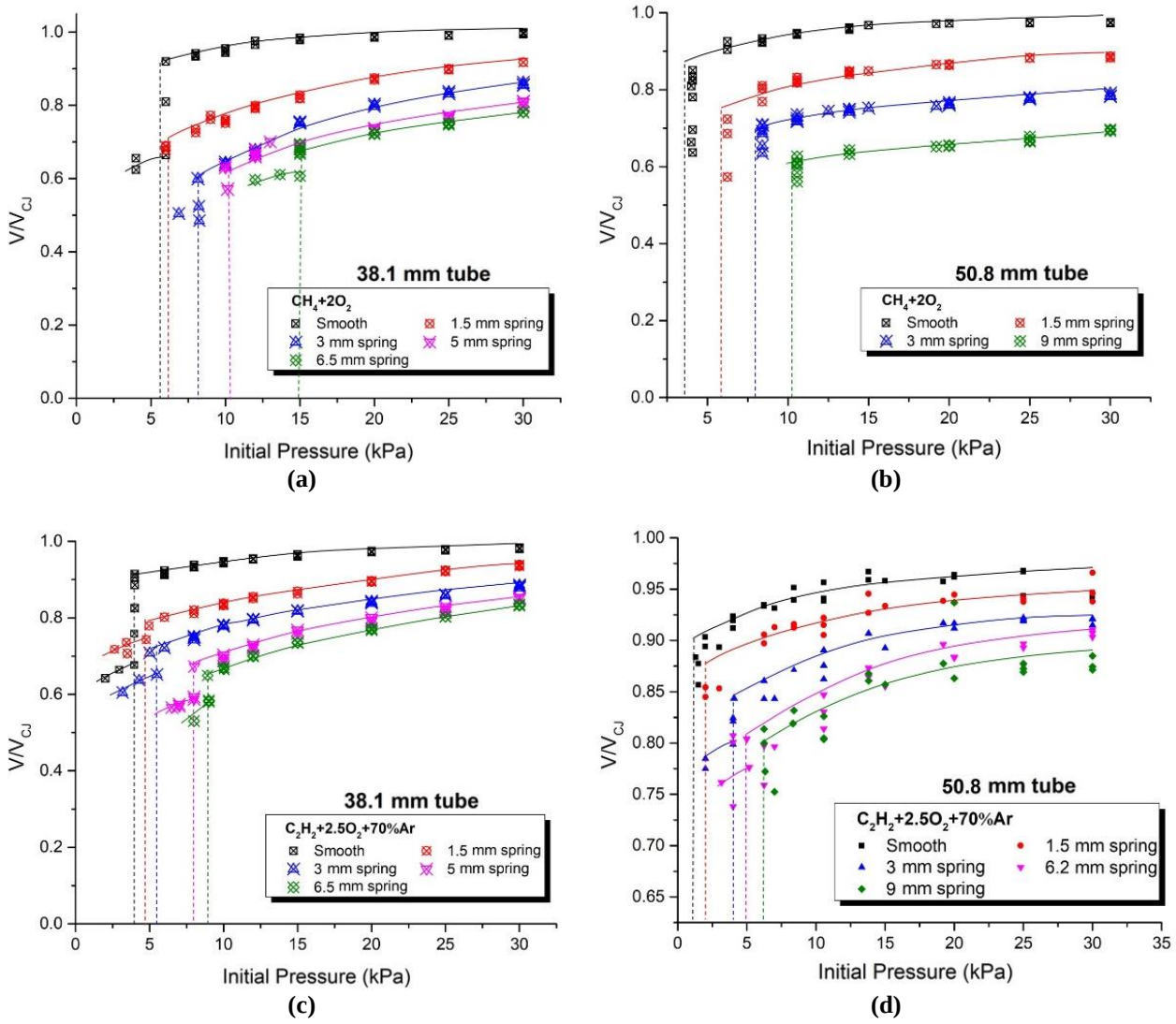

Fig. 4 (continued)

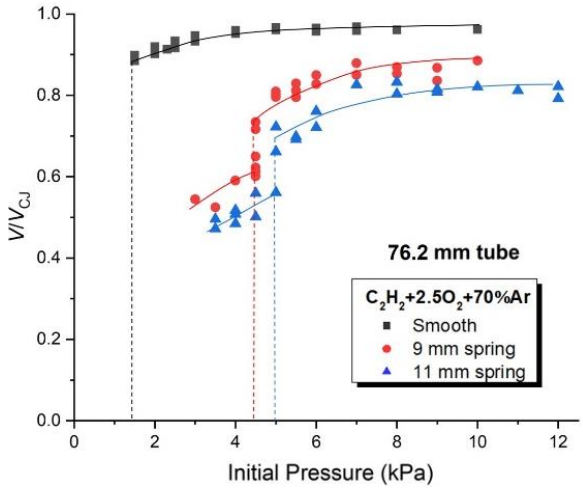
76.2 mm tube
C2H2+2.5O2+70%Ar
Smooth
9 mm spring
11 mm spring
V/VCJ
Initial Pressure (kPa)

(e)

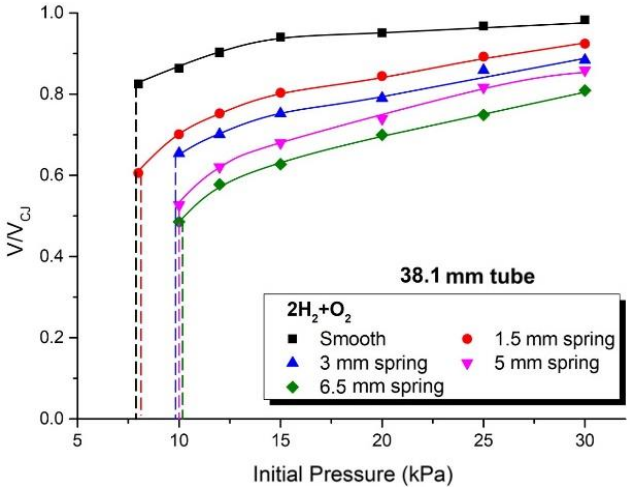
38.1 mm tube
2H2+O2
Smooth
1.5 mm spring
3 mm spring
5 mm spring
6.5 mm spring
V/VCJ
Initial Pressure (kPa)

(f)

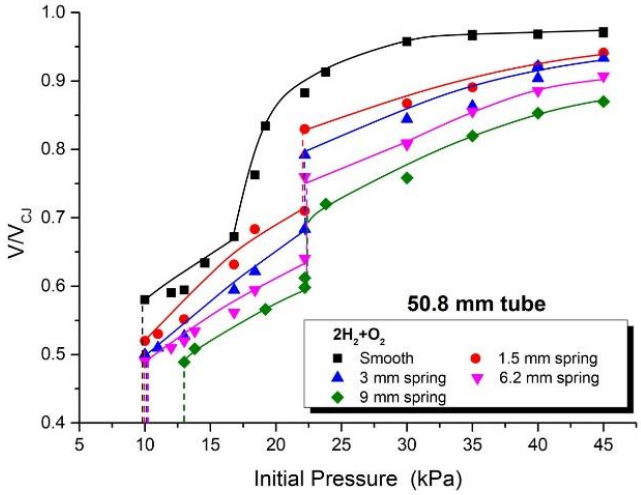
50.8 mm tube
2H2+O2
Smooth
1.5 mm spring
3 mm spring
6.2 mm spring
9 mm spring
V/VCJ
Initial Pressure (kPa)

(g)

Fig. 4

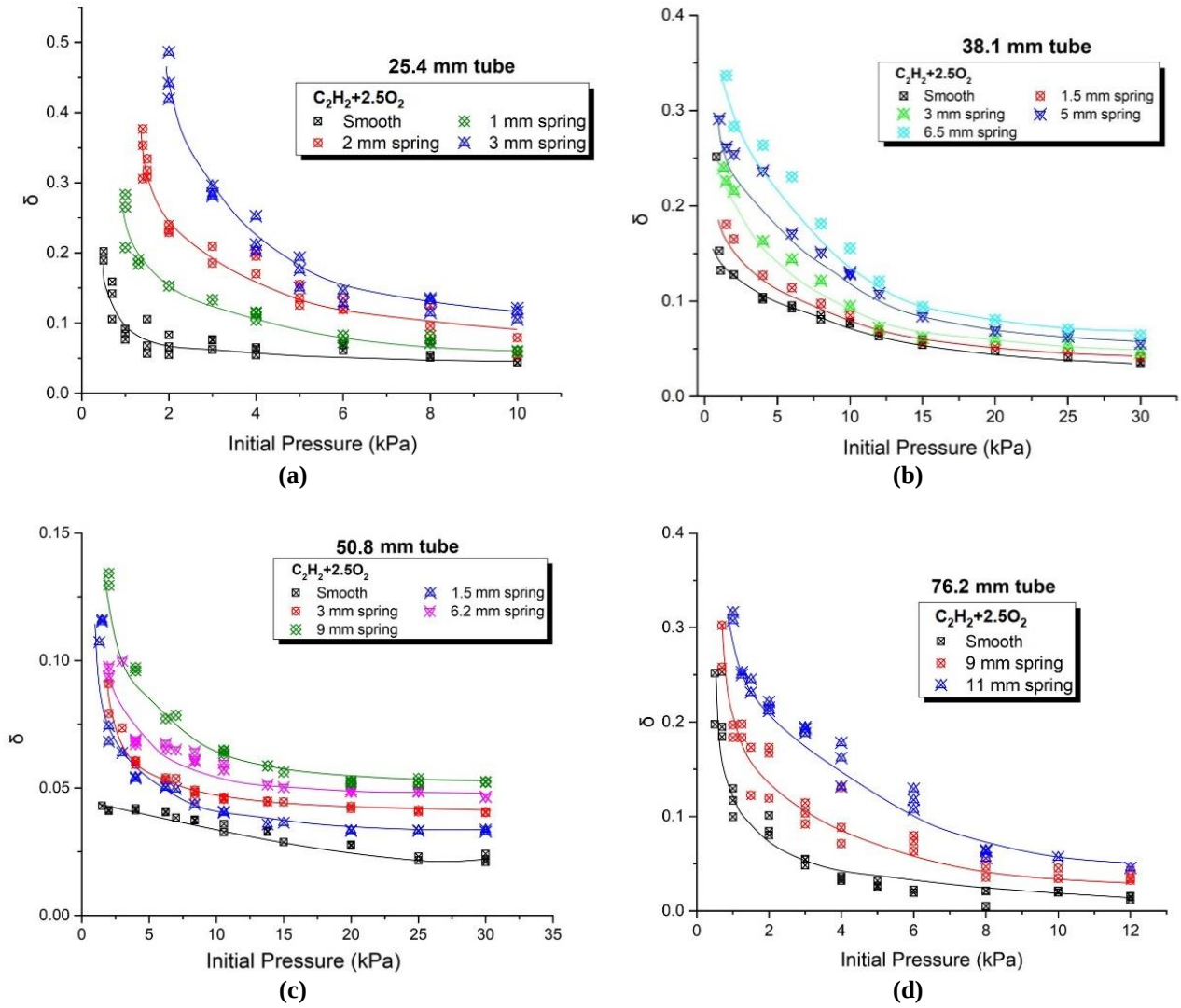
25.4 mm tube
C2H2+2.5O2
Smooth
1 mm spring
2 mm spring
3 mm spring
δ
Initial Pressure (kPa)
(a)
38.1 mm tube
C2H2+2.5O2
Smooth
1.5 mm spring
3 mm spring
5 mm spring
6.5 mm spring
δ
Initial Pressure (kPa)
(b)
50.8 mm tube
C2H2+2.5O2
Smooth
1.5 mm spring
3 mm spring
6.2 mm spring
9 mm spring
δ
Initial Pressure (kPa)
(c)
76.2 mm tube
C2H2+2.5O2
Smooth
9 mm spring
11 mm spring
δ
Initial Pressure (kPa)
(d)

Fig. 5

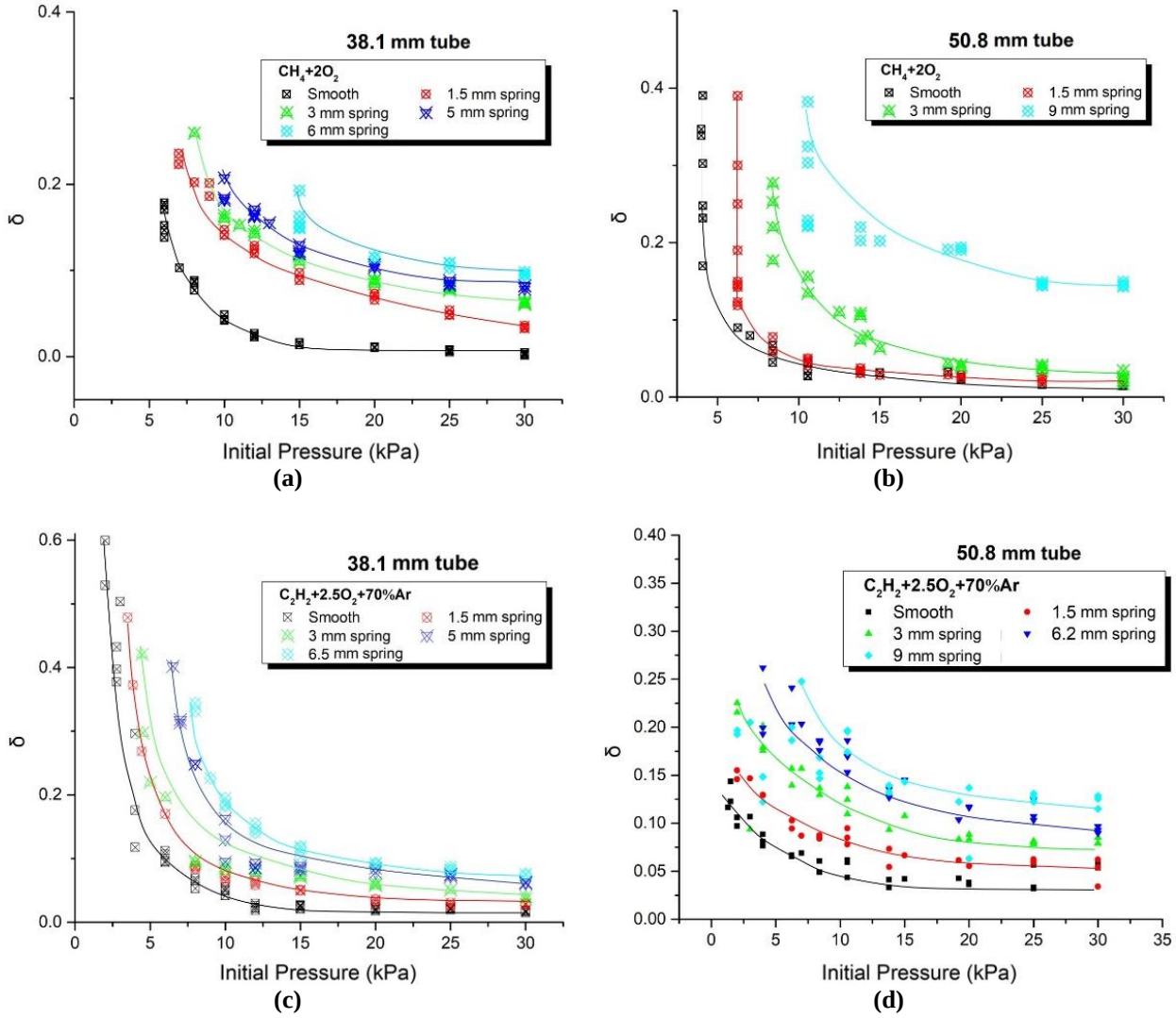

Fig. 6 (continued)

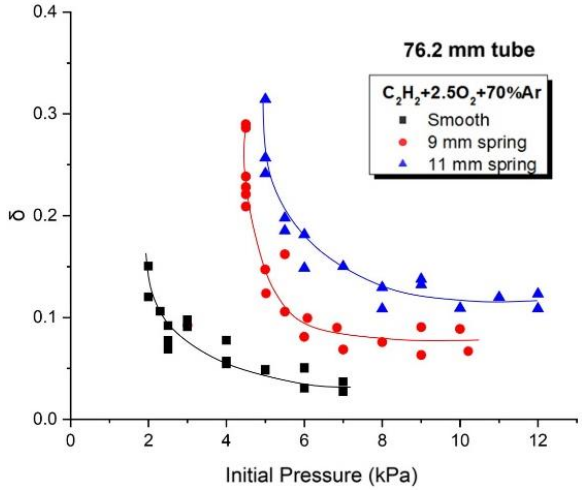
76.2 mm tube
C2H2+2.5O2+70%Ar
Smooth
9 mm spring
11 mm spring
δ
Initial Pressure (kPa)

(e)

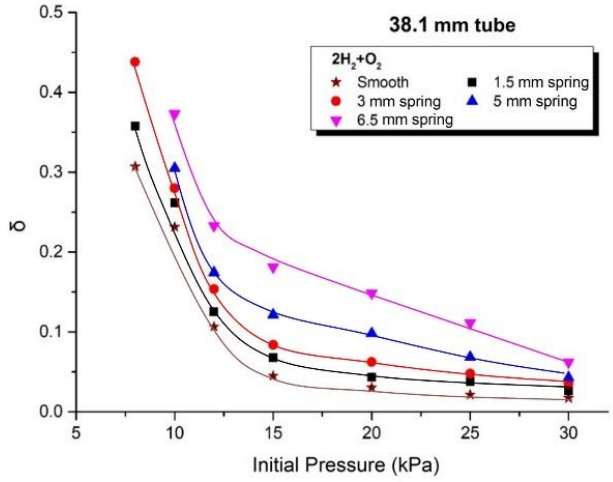
38.1 mm tube
2H2+O2
Smooth
1.5 mm spring
3 mm spring
5 mm spring
6.5 mm spring
δ
Initial Pressure (kPa)

(f)

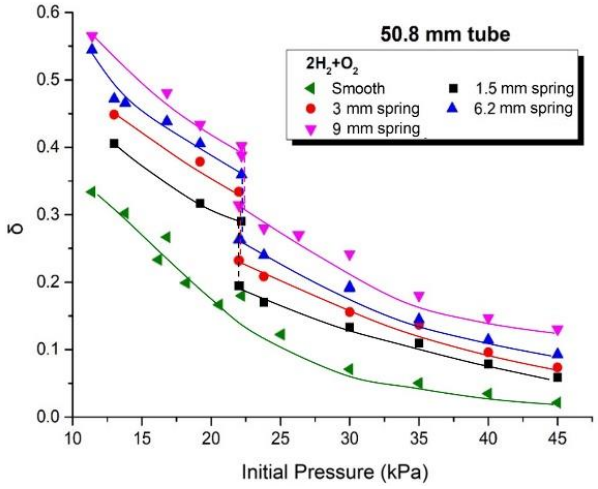
50.8 mm tube
2H2+O2
Smooth
1.5 mm spring
3 mm spring
6.2 mm spring
9 mm spring
δ
Initial Pressure (kPa)

(g)

Fig. 6

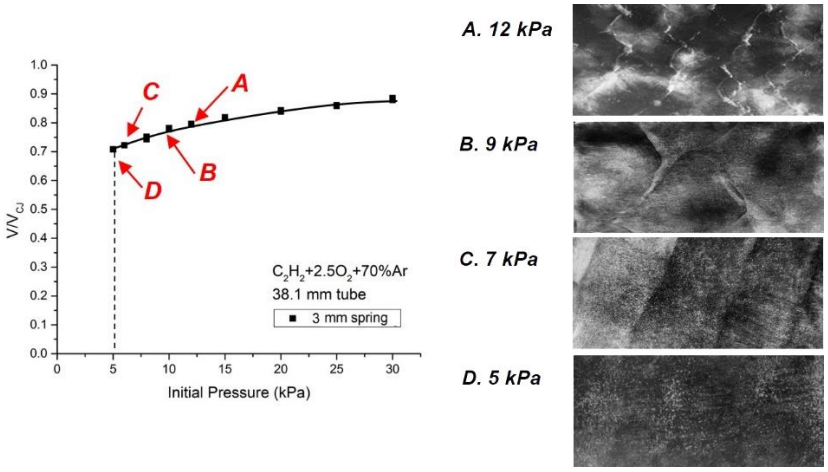
A. 12 kPa
B. 9 kPa
C. 7 kPa
D. 5 kPa
A
B
C
D
V/V_CJ
Initial Pressure (kPa)
C2H2+2.5O2+70%Ar
38.1 mm tube
3 mm spring

(a)

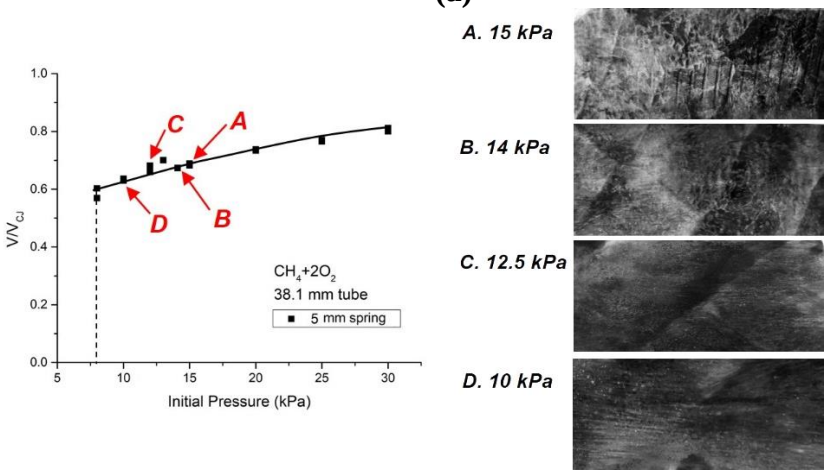
A. 15 kPa
B. 14 kPa
C. 12.5 kPa
D. 10 kPa
A
B
C
D
V/V_CJ
Initial Pressure (kPa)
CH4+2O2
38.1 mm tube
5 mm spring

(b)

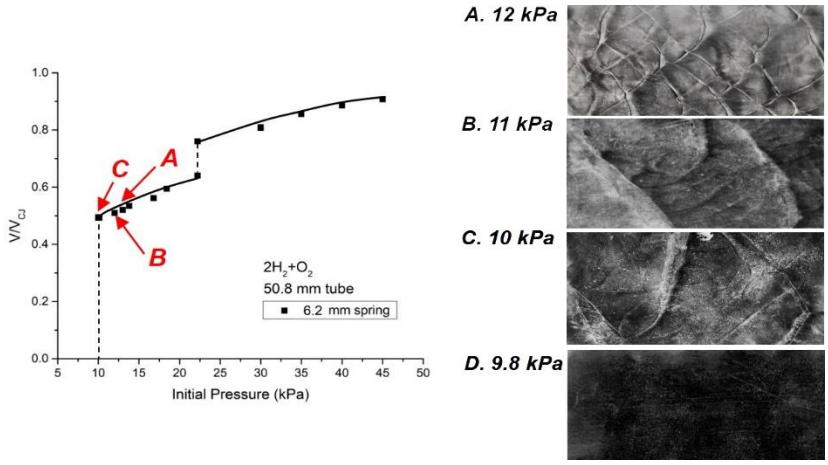
A. 12 kPa
B. 11 kPa
C. 10 kPa
D. 9.8 kPa
A
B
C
V/V_CJ
Initial Pressure (kPa)
2H2+O2
50.8 mm tube
6.2 mm spring

(c)

Fig. 7

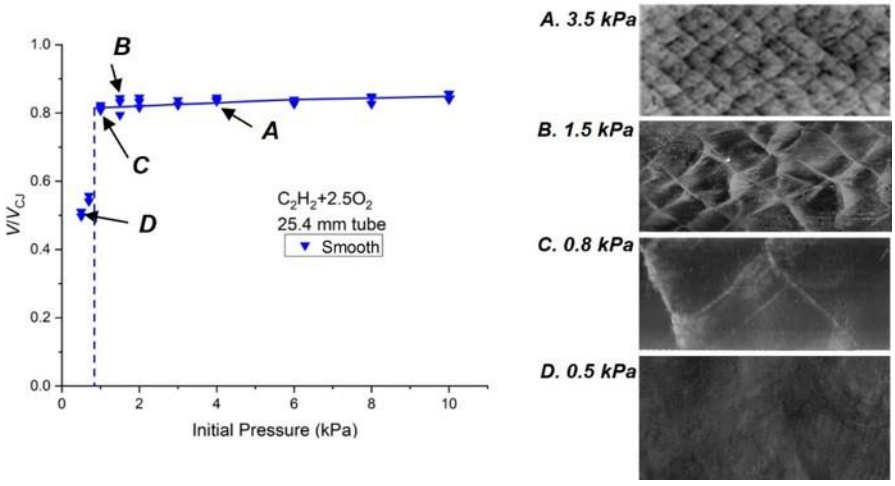
B
A
C
D
C_2H_2+2.5O_2
25.4 mm tube
Smooth
V/V_{CJ}
Initial Pressure (kPa)
A. 3.5 kPa
B. 1.5 kPa
C. 0.8 kPa
D. 0.5 kPa

(a)

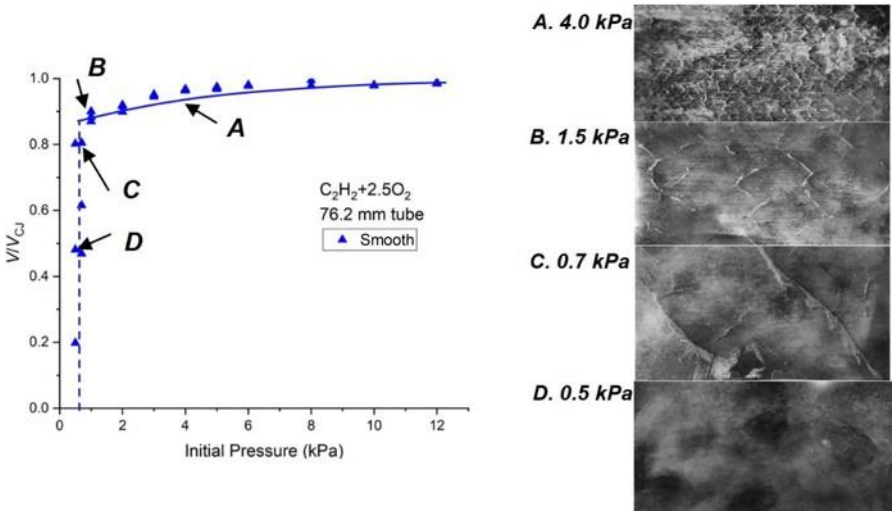
B
A
C
D
C_2H_2+2.5O_2
76.2 mm tube
Smooth
V/V_{CJ}
Initial Pressure (kPa)
A. 4.0 kPa
B. 1.5 kPa
C. 0.7 kPa
D. 0.5 kPa

(b)

Fig. 8

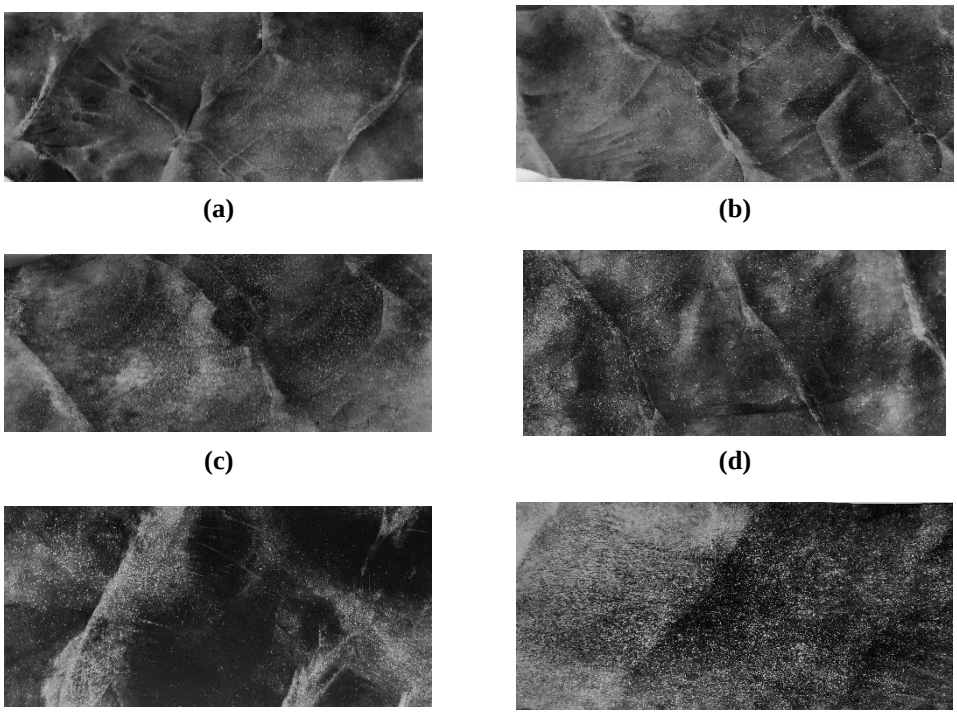

(a) **(b)**

(c) **(d)**

(e) **(f)**

Fig. 9